

Causes and Consequences of Magnetic Field Changes in Neutron Stars

M. Ruderman

*Department of Physics and Columbia Astrophysics Laboratory
Columbia University, New York, NY*

Abstract

Because of the quantum fluid properties of a neutron star core's neutrons and protons, its magnetic field is expected to be coupled strongly to its spin. This predicts a simple evolution of the surface-field of such stars as they spin down or, less commonly, are spun up. Consequences and comparisons with observations are given for properties of solitary spinning down pulsars, including their glitches and spin-down ages, X-ray pulsars, and the formation and pulse characteristics of Millisecond Pulsars. For none of these is there a present conflict between model predictions and what has been observed.

Key words: Pulsar, Magnetic Field, Neutron Star, Glitches

1 Introduction

Enough is understood about the dynamics of the components of a standard (non-magnetar, non-strange) neutron star (NS) to support what should be a reliable description of what happens within a spinning magnetized NS as it ages and spins down or, in rarer cases, when it is spun up.

In a cool core below the crust of a spinning NS superconducting protons coexist with more abundant superfluid neutrons (SF-n) to form a giant atomic nucleus which contains within it a neutralizing sea of relativistic degenerate electrons. The neutrons rotate with a spin-period P (sec) $\equiv 2\pi/\Omega$ only by forming a nearly uniform array of corotating quantized vortex lines parallel to the spin axis, with an area density $n_v \sim 10^4 \text{ cm}^{-2} P^{-1}$. The array must contract

Email address: mar@astro.columbia.edu (M. Ruderman).

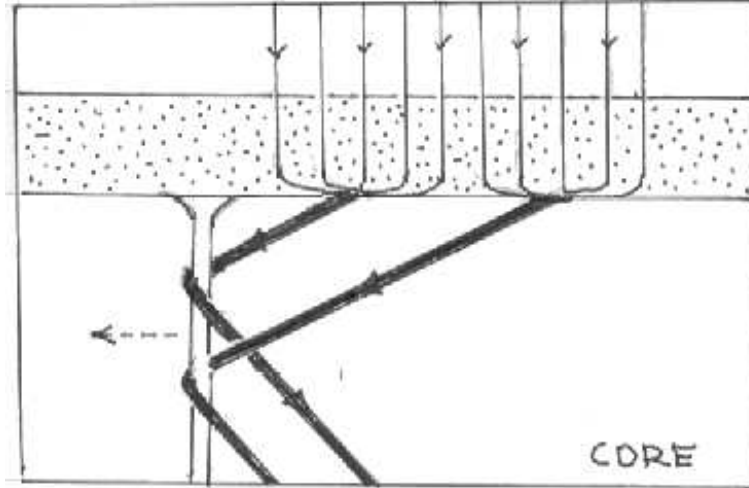


Fig. 1. A moving quantized vortex-line in a NS core’s superfluid neutrons pulling a pair of the core’s proton superfluid quantized flux-tubes anchored in the star’s solid, conducting crust (shown dotted).

(expand) when the NS spins up (down). In stellar core neutron spin-up or spin-down, a vortex a distance r_{\perp} from the spin-axis generally moves outward with a velocity $v_v = r_{\perp}(\dot{P}/2P)$ until r_{\perp} reaches the core’s neutron superfluid radius (R). Any stellar magnetic field passing below the stellar crust must, in order to penetrate through the core’s superconducting protons (SC-p), become a very dense array of quantized flux-tubes ($n_{\Phi} \sim 5 \times 10^{18} B_{12} \text{ cm}^{-2}$ with B the local average magnetic field). Each tube carries a flux $2 \times 10^{-7} \text{ G cm}^2$ and a magnetic field $B_c \sim 10^{15} \text{ G}$.¹ The initial magnetic field within the core of a neutron star is expected to have both toroidal and very non-uniform poloidal components. The web of flux-tubes formed after the transition to superconductivity is then much more complicated and irregular than the neutron vortex-array as well as of order 10^{14} times more dense. Because of the velocity dependence of the short range nuclear force between neutrons and protons, there is a strong interaction between the neutron-superfluid’s vortex-lines and the proton-superconductor’s flux-tubes if they come closer to each other than about 10^{-11} cm . Consequently, when $\dot{P} \neq 0$ flux tubes will be pushed (or pulled) by the moving neutron vortices(29; 30; 24; 6; 25; 9; 14; 28; 31). A realistic flux-tube array will be forced to move along with a changing SF-n vortex array which threads it as long as the force at a vortex-line flux-tube juncture does not grow so large that

¹ This assumes Type II proton superconductivity in the NS core, below the crust, the common result of many calculations. If it were Type I, with many thin regions of $B > \text{several } B_c$, and $B \sim 0$ in between(15), the impact on surface B of changing NS spin proposed below would not change significantly. If, however, $\langle B \rangle$, the locally averaged B inside the NS core exceeds a critical field somewhat greater than B_c , the core’s protons would not become superconducting. This may well be the case for most (or all) “magnetars”(32).

vortex lines cut through flux-tubes. The drag on moving flux-tube arrays from their small average velocities ($\dot{r}_\perp < 10^{-5} \text{cm s}^{-1}$) in spinning-down pulsars, cool (old) enough to have SF-n cores, seems far too small to cause such cut-through.²

The main quantitative uncertainty in the model described below is the maximum sustainable shear-strain ($\theta_m \sim 10^{-4} - 10^{-3}$?) on the conducting crust, which anchors core flux-tubes (cf. Fig 1), before the crust yield-strength is exceeded. An estimate(28) for that maximum sustainable crustal shear-stress, compared to that from the $\langle B^2 \rangle / 8\pi \sim \langle B \rangle B_c / 8\pi$ of the core's flux-tube array, supports a NS model in which the crust yields before the core's flux-tubes are cut through by its moving SF-n vortex array, as long as $B_{12} \gtrsim 1$. Even for much smaller B_{12} , flux-tube anchoring by the conducting crust would result in such cut-through only when the NS's spin-down age ($P/2\dot{P}$) exceeds the crust's Eddy current dissipation time ($\sim 10^7$ yrs.). Then in most observationally relevant regimes the motion of the magnetic flux-tube array near the top of the NS core (and B at the crust surface above it) follows that of the SF-n vortex array which threads it. This forms the basis of a very simple model for describing predicted changes in pulsar magnetic fields during NS spin-up or spin-down which agrees well with a variety of different families of pulsar observations.

2 Magnetic field changes in spinning up neutron stars

NS spin-up, when sustained long enough so that one of the above criteria for relaxation of shear-stress from crust-anchored magnetic flux before cut-through is met, leads to a “squeezing” of surface \mathbf{B} toward the NS spin-axis. After a large decrease in spin-period from an initial P_0 to $P \ll P_0$ all flux would enter and leave the core's surface from the small area within a radius $R(P/P_0)^{1/2}$ of the NS's spin-axis. This surface \mathbf{B} -field change is represented in Figs 2-3 for the special case when the magnetic flux which exits the NS surface from its upper (lower) spin-hemisphere returns to the stellar surface in its lower (upper) one. Potentially observable features of such a “spin-squeezed” surface \mathbf{B} configuration include the following.

- a) A dipole moment nearly aligned along the NS spin-axis.

² Jones(12) has recently found that electron scattering on flux-tube cores allows easier passage of flux-tubes through the SC-p than had been previously estimated (e.g. (25)). In addition, an expected motion-induced flux-tube bunching instability would allow easy co-motion of flux-tubes with the local electron plus SC-p fluid in which they are embedded (26).

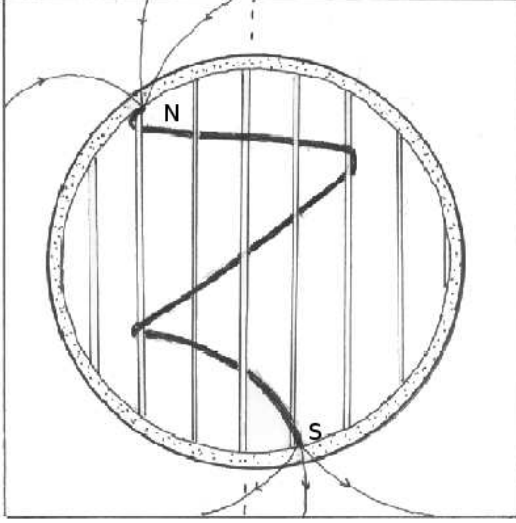


Fig. 2. A single flux-tube (one of 10^{31}) and some of the NS's arrayed vortices (8 of 10^{17}).

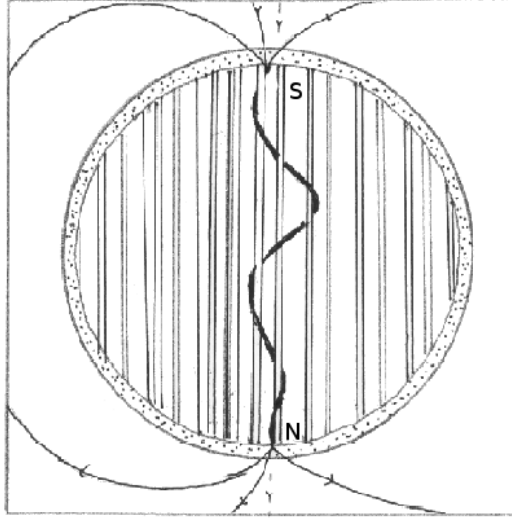


Fig. 3. The flux-tube and vortex array of Fig. 2 after a large stellar spin-up.

- b) A greatly diminished polar cap spanning the “open” field lines when $P/P_0 \rightarrow 0$. For $P < P_0(\Delta/R)(\Omega_0 R/c)^{1/2}$ with Δ the crust thickness ($\sim 10^{-1}R$), the canonical polar cap radius, $r_p \equiv R(\Omega R/c)^{1/2}$, shrinks to $r'_p \equiv \Delta(\Omega R/c)^{1/2}$
- c) A B -field just above the polar cap which has almost no curvature.

If the pre-spin-up surface \mathbf{B} has a sunspot-like configuration (i.e. flux returning to the NS surface in the same hemisphere as that from which it left), the spin-up-squeezed field change is represented in Figs 4 and 5. In this case, potentially observable features when $P \ll P_0$ include the following.

- d) A pulsar dipole moment nearly orthogonal to the NS spin-axis, and
- e) positioned at the crust-core interface.
- f) A dipole moment ($\boldsymbol{\mu}$), or more precisely the component of $\boldsymbol{\mu}$ perpendicular to $\boldsymbol{\Omega}$, reduced from its pre-spin-up size:

$$\frac{\mu_{\perp}(P)}{\mu_{\perp}(P_0)} \sim \left(\frac{P}{P_0}\right)^{1/2}. \quad (1)$$

A more general (and very probably more realistic) pre-spin-up configuration has flux emitted from one spin-hemisphere returning to the stellar surface in both, as in Fig. 6. Spin-up squeezing then typically gives the surface field configuration represented in Fig. 7, a spin-squeezed, nearly orthogonal dipole

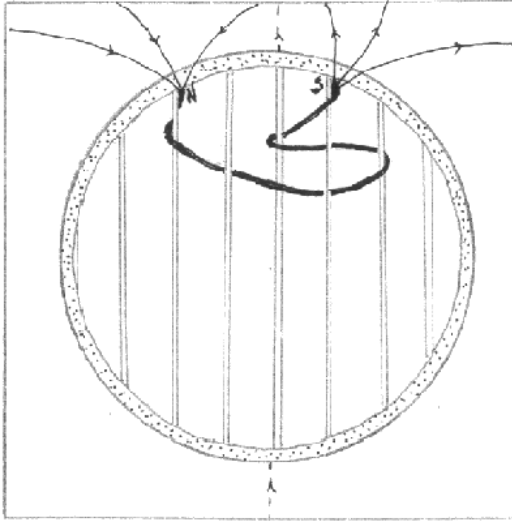


Fig. 4. A single flux-tube, part of a sunspot-like B -field geometry in which flux from a spin-hemisphere of the surface returns to the surface in that same hemisphere.

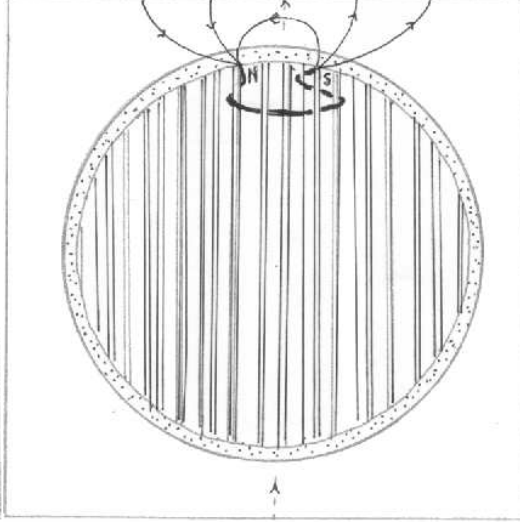


Fig. 5. The flux-tube and vortex array of Fig. 4 after a large stellar spin-up.

on the NS spin-axis with properties (d), (e), and (f), together with an aligned dipole on the spin-axis whose external field is well-represented by North and South poles a distance $2(R - \Delta)$ apart. Further spin-up could lead to the Figs. 8 and 3 configuration; that of Fig. 9 and 5 would be realized only if S_2 of Figs. 6 and 7 is negligible.

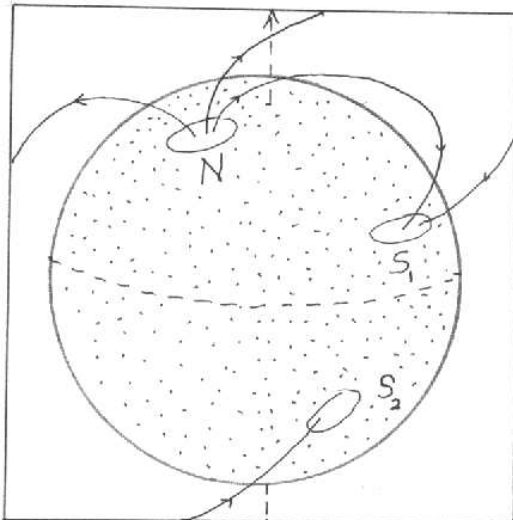


Fig. 6. A surface field which has flux of both Fig. 2 and Fig. 4 configurations.

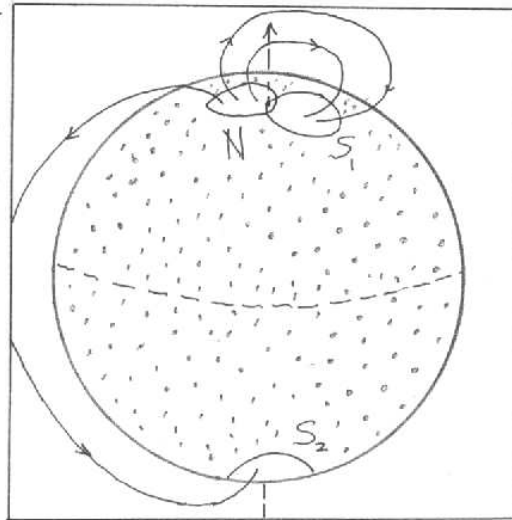


Fig. 7. The field from Fig. 6 after a large stellar spin-up.

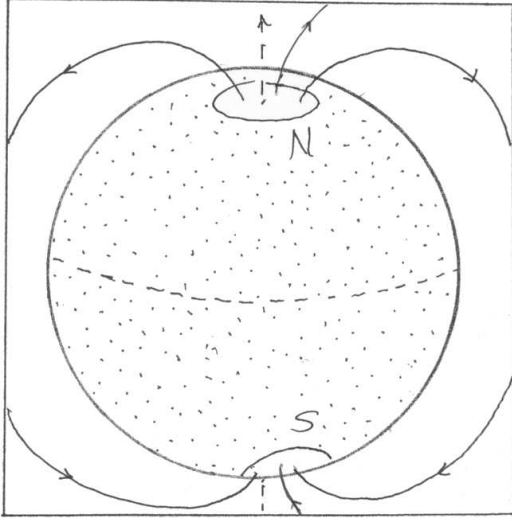


Fig. 8. The field from Fig. 7 after further spin-up.

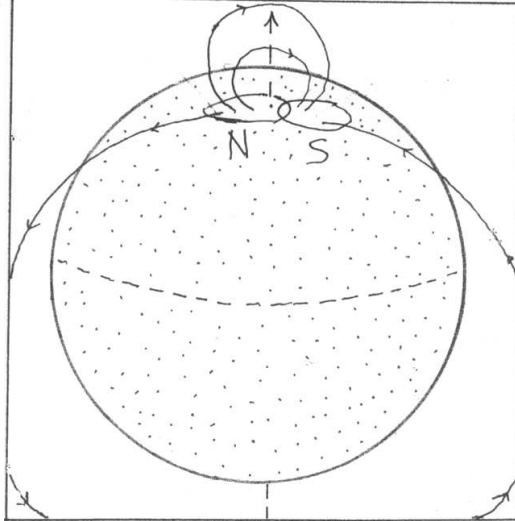


Fig. 9. The field from Fig. 6 after large spin-up when the S_2 contribution to Fig. 7 is negligible.

3 Magnetic field changes in spinning down neutron stars

Consequences of the coupling between a spin-down expansion of a NS's SF-n vortex-array and its SC-p flux-tubes should appear in several observable phases which begin after the NS has cooled enough that the vortex-line array and the flux-tube one have both been formed (typically after about 10^3 yrs.).

- a) As in Eqn (1), except that $P > P_0$, $\mu_{\perp}(P)$ initially grows as $P^{1/2}$. This increase is initially not sensitive to the configuration of surface \mathbf{B} (cf. Fig. 10).
- b) When $P \sim$ several P_0 , a good fraction of a NS's core flux-tubes will have been pushed outwards from the spin-axis to $r_{\perp} \sim R$. These cannot, of course, continue to move outward (Fig. 11) so that Eqn (1) no longer holds. Rather, the mixture of expanding and crust-constrained flux-tubes gives:

$$\frac{\mu_{\perp}(P)}{\mu_{\perp}(P_0)} \sim \left(\frac{P}{P_0}\right)^{\hat{n}} \quad (0 < \hat{n} < 1/2) \quad (2)$$

with the exact value of \hat{n} dependent on details of a core's B -field configuration.

- c) The crust can delay, but not indefinitely prevent, expulsion of this

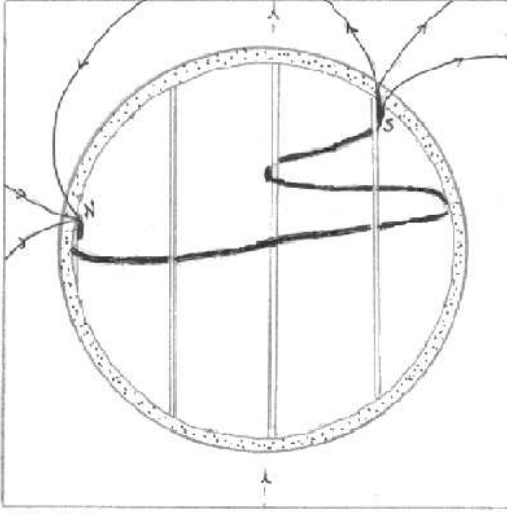


Fig. 10. The flux-tube and vortex-array of Fig. 4 after some spin-down. The expanded configuration would not differ in an important way if it had begun as that of Fig. 2.

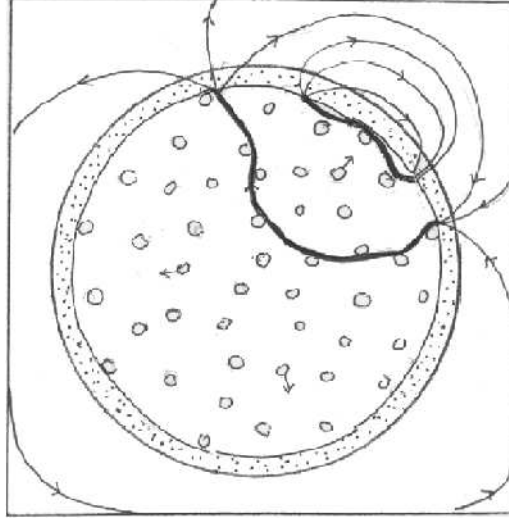


Fig. 11. The equatorial plane, viewed from above, of a configuration like that of Fig. 10, but with two flux-tubes. One tube is being expelled into the crust by the expanded vortex array and will ultimately be eliminated by reconnection.

magnetic field from the NS. When $P \sim$ several P_0 , intertwined vortex plus flux which have been pushed into the core-crust interface will stress the crust enough to exceed its shear-strength (Sect. 4 and Figs. 15 and 16). Then crust movements begin that lead to B -field reconnections. Flux that is threaded by SF-n vortex lines that have not yet reached $r_{\perp} \sim R$, and thus have not yet disappeared in this way, are the remaining source for the NS's dipole moment. The sum of all this remaining flux \propto the total number of remaining vortex-lines ($\propto \Omega$). Then, Eqn (2) holds with $\hat{n} = -1$.

- d) When this remaining B at the crust bottom ($\propto \Omega$) drops to and below $\sim 10^{12}$ G, shear-stress on the crust would no longer be expected to exceed the crust's yield-strength. The NS's surface B may then lag that at the base of its crust by as much as 10^7 yrs., the crust's Eddy current dissipation time.

4 Comparisons of pulsar expectations with model expectations

Fig. 12 shows observationally inferred surface dipole fields (B) as a function of their P for about 10^3 radiopulsars (B is calculated from measured P and \hat{P} , $I\hat{\Omega} = -\mu_{\perp}^2 \Omega^3 c^{-3}$; $B = \mu_{\perp} R^{-3}$ and $I = 10^{45} \text{g cm}^2$). Segments of $B(P)$

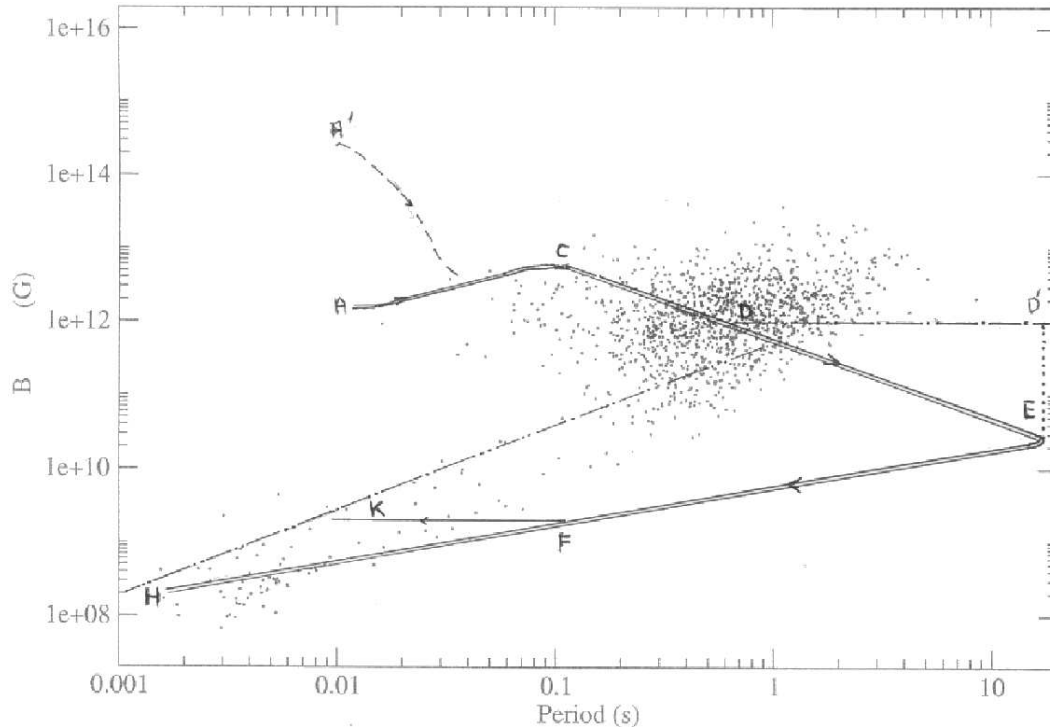


Fig. 12. Dipole- B observed on pulsar surfaces (inferred from measured P and \dot{P}) as a function of pulsar period (P) (12). The solid line segments are the evolutionary segments for B of Sect. 4, based upon the model of Sects. 2 and 3. The dash-dot diagonal is the steady state spin-up line from an accretion disk. The horizontal ($D \rightarrow D'$) is that for a NS surface above a core surface ($D \rightarrow E$).

based upon the model of Sects 2 and 3, are shown for a typical pulsar by the doubled or single solid lines.

- (1) Point A is the (B, P) where, typically, flux-tubes and vortex lines begin coexistence.
- (2) ($A \rightarrow C$) is the expanding array prediction of Sect. 3(b): $B \propto P^{\hat{n}}$ with the model prediction $0 < \hat{n} < 0.5$. The index \hat{n} is known only in the several cases where \dot{P} is also measured: $\hat{n} = +0.3, 0.1, 0.6, 0.1$ (20; 13; 35; 3).
- (3) ($C \rightarrow D$) is the flux-expulsion and continual reconnection segment of Sect. 3(e). The model predicts $\langle \hat{n} \rangle = -1$ for \hat{n} averaged over the ($C \rightarrow D$) history of any one pulsar. Reliable \dot{P} are not generally measurable in this (B, P) region. However comparison of the spin-down times $P/2\dot{P}$ with actual pulsar ages, inferred from probable distance traveled since birth(5), give $\langle \hat{n} \rangle = -0.8 \pm 0.4$, not inconsistent with the model prediction.
- (4) ($D \rightarrow E$) is the core-surface/crust-base B evolution for $\sim 10^{10}$ yrs. The horizontal ($D \rightarrow D'$) is the NS crust's surface field, remaining near 10^{12}

G for $\sim 10^7$ yrs. as discussed in Sect. 3(d). This segment should be characteristic of typical “X-ray pulsars” (NSs in binaries spun up or down by active companions through a wide range of P (e.g. Hercules X-1 with $P \sim 1$ s to Vela X-1 with $P \sim 10^3$ s) until crustal Eddy current decay allows a ($D' \rightarrow E$) decay from some D' region.

A small minority of NSs, after ($D' \rightarrow E$) segments, will be resurrected by accretion from a previously passive White Dwarf companion which now overflows its Roche lobe (LMXBs). These NSs have entered into the spin-up phase of Sect. 2 until they reach a steady state on the canonical “spin-up line” represented by the dot-dashed diagonal of Fig. 12 (for $\dot{M} = 10^{-1} \dot{M}_{Eddington}$).

- (5) ($E \rightarrow F \rightarrow H$) is the spin-up segment when the NS surface B has the sunspot geometry of Figs. 4, 5, and 9, which allows spin-up to minimal P before spin-up equilibrium is reached. Observations of maximally spun-up millisecond pulsars (MSPs) support the Sect. 2 model for such MSP formation: Sect. 2(d)’s high fraction of MSPs with two subpulses 180° apart, characteristic of orthogonal rotators(5; 27; 11; 4; 1); Sect. 2(e)’s B -field geometry, from linear polarization and its frequency dependence in such subpulses(4).
- (6) ($E \rightarrow F \rightarrow K$) is the track of surface B (here the total dipole field) predicted after large spin-up from (E) with Fig. 6 geometry to (F) with Fig. 7 geometry. Further spin-up diminishes only the orthogonal component of $\boldsymbol{\mu}$ until an almost aligned rotator (Figs. 3 and 8) results when (K) is reached. X-ray emission from the almost aligned MSP PSR 0437 ($P = 6$ ms) supports a (predicted) tiny polar cap area about $(\Delta/R)^2 \sim 10^{-2}$ that from a central dipole moment configuration for the same P (Sect. 2(b) and refs (4; 27; 1)).

Expected consequences for pulsar dipole- \mathbf{B} changing according to the Sects. 2-3 model and Fig. 12 are supported by many kinds of observations. However, for almost all there is usually another popular explanation (e.g. B getting from (D) to (H) just by burial of \mathbf{B} by accreted matter from a companion(33; 2; 36)).

5 Pulsar spin-period glitches from spin-induced B -field changes

Moving core flux-tubes continually build up shearing stress in the conducting crust which anchors B -field that traverses it. If this stress grows to exceed the crust’s yield strength, subsequent relaxation may, at least partly, be through relatively sudden crustal readjustments (“crust-breaking”). Such events would

GLITCHES

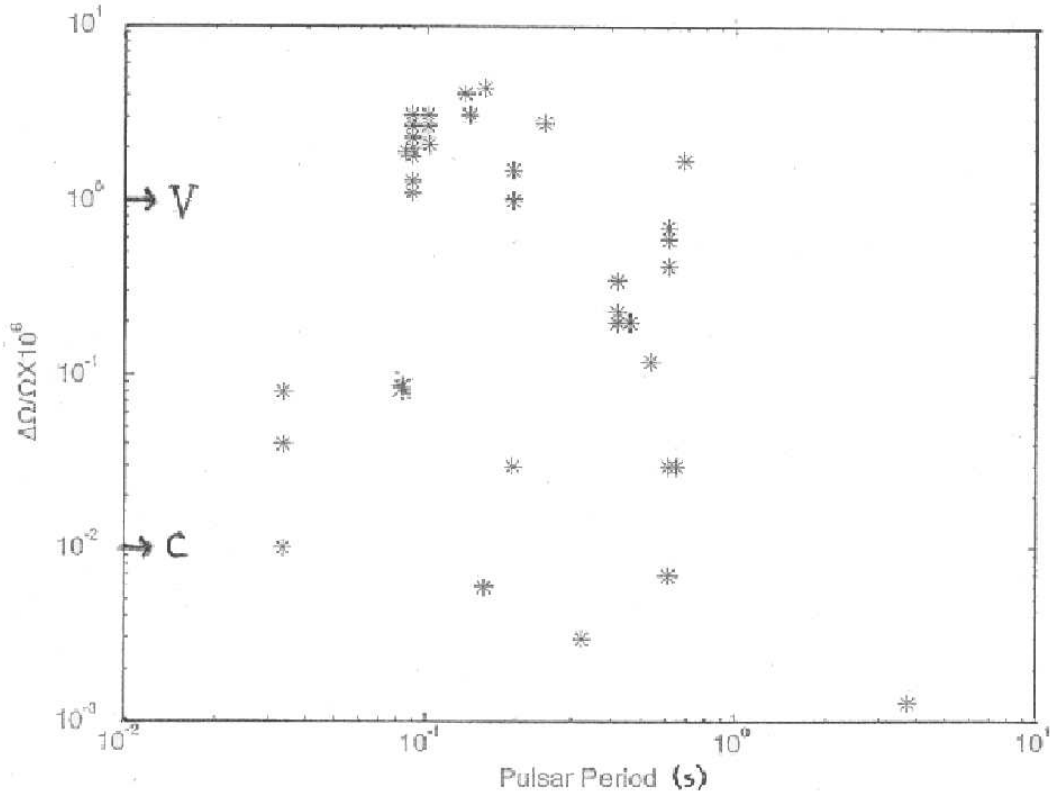


Fig. 13. Observed jumps (“glitches”) in pulsar spin-rates ($\Delta\Omega/\Omega$) of pulsars with various periods (P). The Vela-like family (**V**) has $\Delta\Omega/\Omega \sim 10^{-6}$. The Crab-like one (**C**) has $\Delta\Omega/\Omega \sim 10^{-7} - 10^{-8}$ (19; 16; 8; 34; 7).

cause very small spin-up jumps in spinning-down NSs (spin-period “glitches”). The Sect. 2-3 model for the evolution of a core’s flux-tube array suggests glitch details in pulsars similar to those of the two observed glitch families: Crab-like glitches (**C**) and the very much larger giant Vela-like ones (**V**) of Fig. 13.

- a) *Crab-like glitches* In both the ($A \rightarrow C$) and ($C \rightarrow D$) segments of Fig. 12, an expanding quasi-uniform vortex-array carries a flux-tube array outward with it. If growing flux-tube-induced stress on the crust is partly relaxed by “sudden” outward crust movements (of magnitude s) where the stress is strongest (with density preserving backflow elsewhere in the stratified crust) the following consequences are expected:

- (1) a “sudden” permanent increase in μ_{\perp} , spin-down torque, and $|\dot{\Omega}|$: $\Delta\dot{\Omega}/\dot{\Omega} \sim s/R \sim \Delta\theta$ (strain relaxation) $\lesssim \theta_{\max} \sim 10^{-3}$. (This is the largest non-transient fractional change in any of the pulsar observables expected from “breaking” the crust.) A

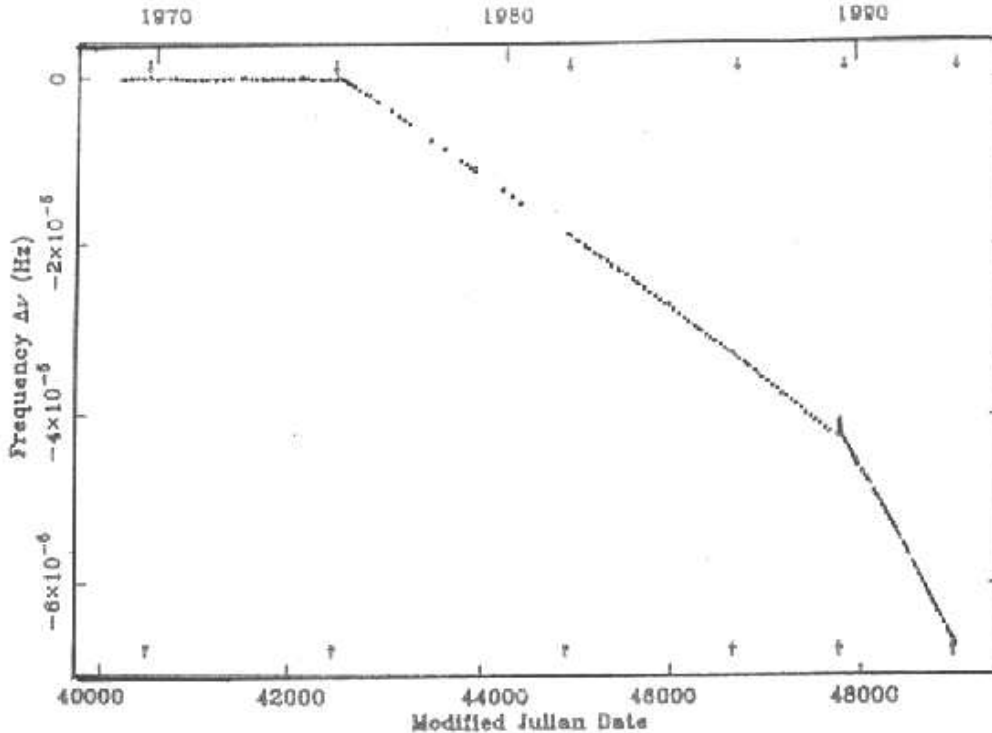


Fig. 14. The difference between Crab pulsar periods observed over a 23 yr interval and those predicted from extrapolation from measurement of P , \dot{P} , and \ddot{P} at the beginning of that interval. These “sudden” permanent fractional jumps in spin-down rate ($\Delta\dot{\Omega}/\dot{\Omega} \sim +5 \times 10^{-4}$) occur at glitches ($\Delta\Omega/\Omega \sim 10^{-8} - 10^{-7}$) but are 10^4 times greater in magnitude(18; 17).

permanent glitch-associated jump in NS spin-down rate of this sign and magnitude ($\sim 3 \times 10^{-4}$) is indeed observed in the larger Crab glitches (Fig. 14)(19; 16; 8; 34).

- (2) a “sudden” reduction in shear stress on the crust by the flux-tubes attached to it from below. This is matched by an equivalent reduction in pull-back on the core’s expanding vortex array by the core flux-tube array attached to it. The n-vortices therefore “suddenly” move out to a new equilibrium position where the Magnus force on them is reduced by just this amount. The high density SF-n sea therefore spins down a bit. All the (less dense) charged components of the NS (crust, core-p and-e) together with the flux-attached n-vortex-array spin-up much more. (The total angular momentum of the NS does not change significantly in the brief time for development of the glitch.) A new equilibrium is established in which the charged components (all that can be observed, of course, is P of the crust’s surface) have been spun up. For Crab B and P , the estimated(26)

$\Delta\Omega/\Omega \sim 10^{-4}(\Delta\dot{\Omega}/\dot{\Omega})$, consistent with both the relatively large Crab glitches of Fig. 14 and also with much smaller Crab glitches not shown there(34).

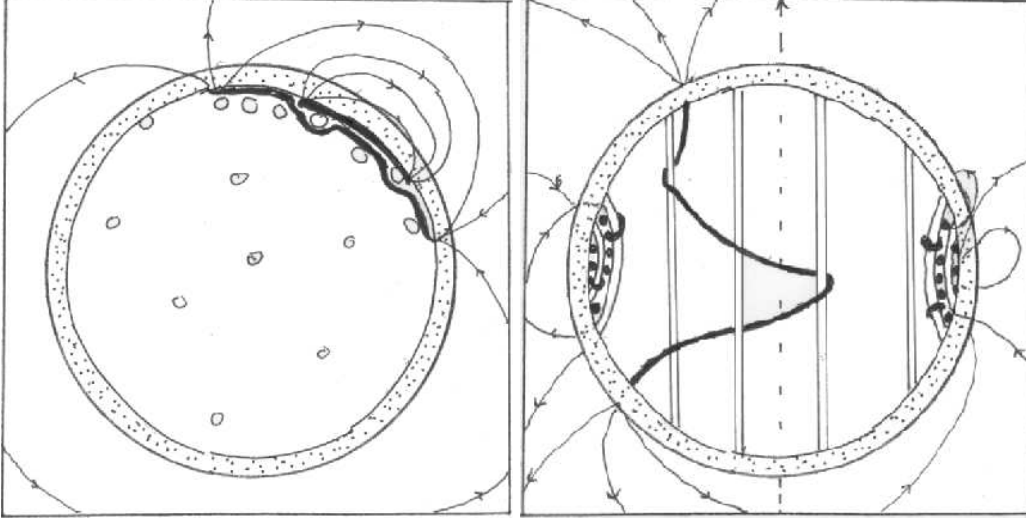


Fig. 15. The configuration (top view) of Fig. 11 after further spin-down. Flux-tubes are piling up in an equatorial annulus at the core-crust interface. The blocked flux-tubes, in turn, block short segments of vortex lines which forced them into this annulus.

Fig. 16. A side view of the representation of the Fig. 15 configuration with the addition of one flux-tube, which the expanding vortex-array has not yet forced out to a radius $\sim R$.

b) *Giant Vela-like (V) glitches*. The second (V)-family of glitches differs from that of Crab-like ones (C) in several ways.

- (1) $(\Delta\Omega/\Omega)_V \sim 10^2 \times (\Delta\Omega/\Omega)_C$.
- (2) V-glitches develop their $\Delta\Omega$ in less than 10^2 sec.: the $\Delta\Omega$ of a V-glitch is already decreasing in magnitude when first resolved(16), while C-glitches are still rising toward their full $\Delta\Omega$ for almost 10^5 sec(7; 21).
- (3) V-glitches are observed in pulsars (mainly, but not always) in Fig. 12 along $(C \rightarrow D)$ while C-glitches are observed all along $(A \rightarrow C \rightarrow D)$.
- (4) The C-glitch proportionality between $\Delta\dot{\Omega}/\dot{\Omega}$ and $\Delta\Omega/\Omega$ would

greatly overestimate $(\Delta\dot{\Omega}/\dot{\Omega})$ for V-glitches.

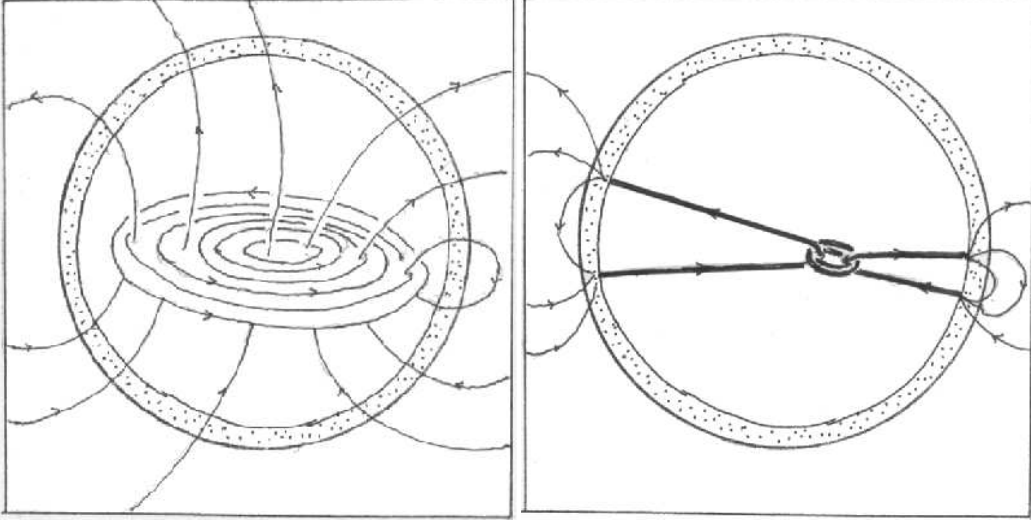


Fig. 17. A schematic representation of a young NS's magnetic field just before the NS cools to the transition temperature for proton superconductivity. Some shearing stress preventing an even more stabilized configuration is probably borne by the NS crust which solidified much earlier.

Fig. 18. A representation of the Fig. 17 magnetic field after core flux-tube formation and relaxation to a new quasi-equilibrium. The initially increased stress in the crust (cf. Fig. 1) is assumed to exceed the crust's shear-stress yield strength. A later formation of SF-n vortex-lines would halt such relaxation.

The existence of a second glitch family, with V-properties, is expected from a second effect of vortex-driven flux-tube movement in a NS core. If there were no very dense, comoving, flux-tube environment around them, outward moving core-vortices could smoothly shorten and then disappear entirely as they reached the core's surface at its spin-equator. (We ignore crustal SF-n here.) However, the strongly conducting crust there resists entry of the flux-tubes which the vortices also bring with them to the crust's base. This causes a pile-up of pushed flux-tubes into a small equatorial annulus (Figs. 15 and 16) which delays the final vortex-line disappearance. The vortex movement in which they vanish occurs either in vortex-line flux-tube cut-through events, or, more likely, in a sudden breaking of the crust which has been overstressed by the increasing shear-stress on it from the growing annulus. Giant V-glitches were proposed as such events(26; 28), allowing a "sudden" reduction of part of this otherwise growing annulus of excess angular momentum and

also some of the magnetic flux trapped within it. These would not begin until enough vortex-lines, initially distributed almost uniformly throughout the core, have piled up in the annulus for the flux-tubes they bring with them to supply the needed shear stress. Estimates of V-glitch $\Delta\dot{\Omega}/\dot{\Omega}$ magnitudes are less reliable than those for C-glitch ones. A very rough one, based upon plausible guesses and an assumed Ω/R about the same as those in the larger C-glitches, suggest V-glitch repetition rates and magnitudes not unsimilar to observed ones(28; 26).

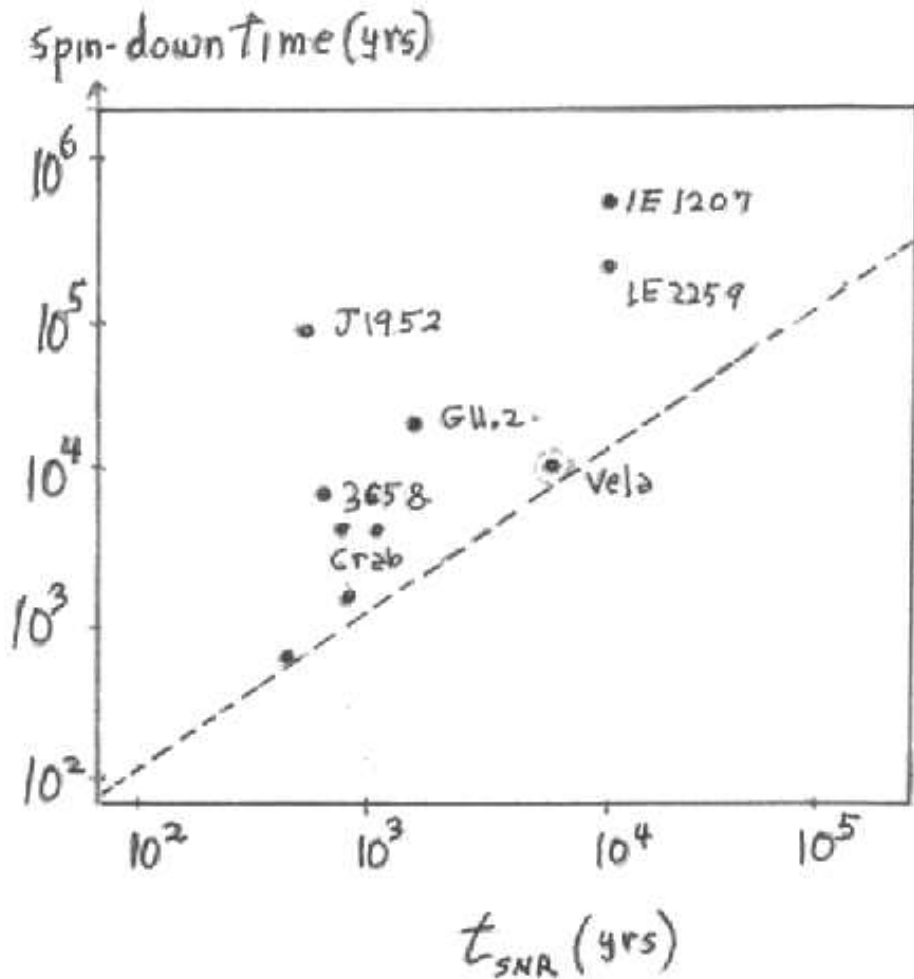


Fig. 19. Observed spin-down times for pulsars ($P/2\dot{P}$) vs the time since birth of these same pulsars as inferred by the ages of the supernova remnants in which they are still embedded (t_{SNR})(28; 23).

6 In the beginning

The proposed spin-down biography of a NS surface B presented in Sects. 3,4, and 5 began at (A) (or perhaps A') in Fig. 12 when that typical NS is expected to be about 10^3 yrs old. Before that its crust had solidified (age \sim a minute), its core protons had become superconducting (~ 1 yr?), and core neutrons became superfluid ($\sim 10^3$ yrs?). If so, there would be a nearly 10^3 year interval between formation of the NS core's magnetic flux-tube array and control of that array's movement by that of a SF-n vortex array. During that interval an early magneto-hydrodynamic equilibrium involving poloidal and toroidal fields, and some crustal shear stress (Fig. 17) would be upset by the dramatically altered B -field stresses after flux-tube formation(28). The subsequent jump in shearing stress on the crust surface B change. The recent reconsideration of drag on moving flux-tubes(12) suggests the core flux-tube adjustment can take $\sim 10^3$ yrs. For many NSs, depending on historical details of their B structure, dipole moments should become much smaller (Fig. 18). Their post-partem values and subsequent expected drops in their sizes have been estimated and proposed (28) as the reason many young pulsars have spin-down ages ($P/2\dot{P}$) up to 10^2 times greater than their true ages (Fig. 19).

7 Acknowledgements

I am happy to thank E.V. Gotthelf, J.P. Halpern, P. Jones, J. Sauls, J. Trumper, and colleagues at the Institute of Astronomy (Cambridge) for helpful discussions.

References

- [1] Becker, W. & Aschenbach, B. 2002, "X-ray Observations of Neutron Stars", Proc. 270 WE-Heraeus Seminar, eds. W. Becker, H. Lesch, J. Trumper, MPE Rpt. 278, astro-ph/0208466.
- [2] Burderi, L. & D'Amico 1997, ApJ, 490, 343.
- [3] Camilo, F. et al. 2000, ApJ, 541, 367.
- [4] Chen, K., & Ruderman, M. 1993, ApJ, 408, 179.
- [5] Cordes, J. & Chernoff, D. 1998, ApJ, 505, 315.

- [6] Ding, K., Cheng, K.S., & Chau, H., 1993 ApJ, 408, 167.
- [7] Flanagan, C. 1990, Nature, 345, 416; McCulloch, P., Hamilton, P., McConnel, D., & King, E. 1990, Nature, 346, 822.
- [8] Gullahorn, G., Isaacman, R., Rankin, J., & Payne, R. 1977, AJ, 81, 309.; Demianski, M. & Prószyński, M. 1983, MNRAS, 202, 437.
- [9] Jahan-Miri, M. 2000 ApJ, 532, 514.
- [11] Jayawardhana, R. & Grindlay, J. 1995, J. Astron. Soc. Pac. Conf. Ser., 105, 231.
- [11] Jayawardhana, R. & Grindlay, J. 1995, J. Astron. Soc. Pac. Conf. Ser., 105, 231.
- [12] Jones, P. 2005 MNRAS, *to be published*.
- [13] Kaspi, V., Manchester, R., Siegman, B., Johnston, S., & Lyne, A. 1994, ApJ, 422, 544, L177.
- [14] Konenkov, D. & Geppert, U. 2001 MNRAS,325, 426.
- [15] Link, B. 2003, Phys. Rev. Lett., 91, 101101.
- [16] Lyne, A., Graham-Smith, F., & Pritchard, R., 1992, Nature, 359, 706.
- [17] Lyne, A., Pritchard, R., & Graham-Smith, F. 1993, MNRAS, 265, 1003.
- [18] Lyne, A., Pritchard, R., & Shemar, S. 1995, J. Astrophys. Astr., 16, 179.
- [19] Lyne, A., Pritchard, R., Graham-Smith, F., & Camilo, F. 1996, Nature, 381, 497.
- [20] Lyne, A., Pritchard, R., & Graham-Smith, F. 1998, MNRAS 233, 267.
- [21] Lyne, A., Shemar, S., & Graham-Smith, F. 2000, MNRAS, 315, 534.
- [22] Manchester, R. 2004, Science, 304, 489.
- [23] Marshall, F., Gotthelf, E., Middleditch, J., Wang, Q., & Zhang, W. 2004, ApJ, 603, 572;
- [24] Ruderman, M. 1991 ApJ 366, 261 and ApJ, 382, 576.

- [25] Ruderman, M., Zhu, T., & Chen, K., 1998 ApJ, 492, 267 and 493, 397.
- [26] Ruderman, M. 2004 in *From X-Ray Binaries to Gamma-Ray Bursts*, ed. E. van den Heuvel, L. Kapper, E. Rol & R. Wijers, ASP conf. Series 308, 251.
- [27] Ruderman, M. 2004 in *X-ray and γ -ray Astrophysics of Galactic Sources*, Proc. 4th Agile Science Workshop, 2003, ed. M. Tavani, A. Pellizoni, & S. Vercellone, IASF.
- [28] Ruderman, M. 2005, astro-ph/0410607, 2004 ASI Neutron Star Workshop (in press).
- [29] Sauls, J., 1989 in *Timing Neutron Stars*, H. Ögelman and E. van den Heuvel, eds. Dordrecht: Kluwer.
- [30] Srinivasan, G., Bhattacharya, D., Muslimov, A., and Tsygan, A. 1990 Curr. Sci., 59, 31.
- [31] Srinivasan, G. 2005, *these Proceedings*.
- [32] Thompson, R., & Duncan, R., ApJ, 473, (1996) 322.
- [33] van den Heuvel, E., & Bitzaraki, O. 1995, A&A, 297L, 41V.
- [34] Wong, J., Backer, D., & Lyne, A. 2001, ApJ, 548, 477.
- [35] Zhang, W., Marshall, F., Gotthelf, E., Middleditch, J., & Wang, Q. 2001, ApJ, 544, L177.
- [36] Zhang, C., & Kojima, Y. 2005, MNRAS, *in press*.